Theor Appl Climatol (2017) 127:17–29
DOI 10.1007/s00704-015-1614-8

ORIGINAL PAPER

High temperature extremes in the Czech Republic 1961–2010 and their synoptic variants

A. Valeriánová[1] · L. Crhová[1,2] · E. Holtanová[1,2] · M. Kašpar[3] · M. Müller[3,4] · J. Pecho[3,5]

Received: 28 January 2015 / Accepted: 20 August 2015 / Published online: 3 September 2015

Abstract Our research focuses on the analysis of extreme high maximum air temperature events (EXHTEs) in the Czech Republic in the period 1961–2010, their climatological characteristics, and on the identification of synoptic-scale circulation conditions conductive to them. EXHTEs are detected using the Weather Extremity Index (WEI) combining return periods of daily maximum air temperature, duration of events, and the extent of the affected area. We selected 37 EXHTEs as non-overlapping periods with the highest WEI. Some long EXHTEs were divided into several shorter synoptically homogeneous episodes. Using the two-level divisive clustering of 700 hPa air temperature and wind field anomalies, we obtained four main variants of synoptic-scale circulation conditions. The most frequent variant associated with extreme episodes is characterized by a westerly flow connected with a high pressure ridge extending northeastward from North Africa over Central Europe or with an anticyclone centered over the Central Mediterranean. The most extreme episodes occurred during the variant characterized by an easterly flow between a high pressure area to the northeast and a low pressure area to the southeast.

✉ A. Valeriánová
anna.valerianova@chmi.cz

[1] Czech Hydrometeorological Institute, Prague, Czech Republic

[2] Faculty of Mathematics and Physics, Charles University in Prague, Ke Karlovu 3, 12116 Prague, Czech Republic

[3] Institute of Atmospheric Physics, Academy of Sciences, Boční II, 1401, 14131 Prague, Czech Republic

[4] Faculty of Science, Charles University in Prague, Albertov 6, 12843 Prague, Czech Republic

[5] Technical University Liberec, Liberec, Czech Republic

1 Introduction

The Czech Republic (CZ) is located in Central Europe and characterized by a complex orography with elevations varying from 115 to 1602 m above sea level (Fig. 1). The area of the CZ lies in the temperate climate zone on the border between the oceanic and continental temperate climate (Trewartha and Horn 1980; Belda et al. 2014). The continentality of the climate increases from west to east (Tolasz et al. 2007). Mean annual near surface air temperature varies from 1 °C at the top of the highest mountains to app. 10 °C in the lowland areas of central Bohemia and southern Moravia. The monthly mean air temperature of the warmest month (typically July or August) is between 10 and 20 °C. Average annual maximum air temperature varies from 26 to 35 °C in most of the area of the CZ (Tolasz et al. 2007). The highest value of maximum daily air temperature on record in the CZ (40.4 °C) was detected on 20 August 2012 at the Dobřichovice station located in central Bohemia (Holtanová et al. 2014). During recent decades, a positive trend in various air temperature characteristics has been observed in the CZ (Brázdil et al. 2009).

Extremely high air temperature is associated with many negative impacts, e.g., higher energy demand for air conditioning, risk of power failure, and an increased rate of sickness and mortality (e.g., Beniston et al. 2007; Kyselý 2010; Kyselý and Plavcová 2012). The most notable examples of such extreme high air temperature events are the heat wave in July–August 2003 in central-western Europe (in particular France, Italy, and Britain) and in July–August 2010 in central-western Russia. Both are considered as the major climate anomalies in the extratropics in the recent times (the most extreme in 500 years with more than 70,000 additional deaths in 2003 and 50,000 in 2010). The main features that characterized the extreme heat waves in 2003 and 2010 from meteorological, climatological, environmental, and health-mortality view

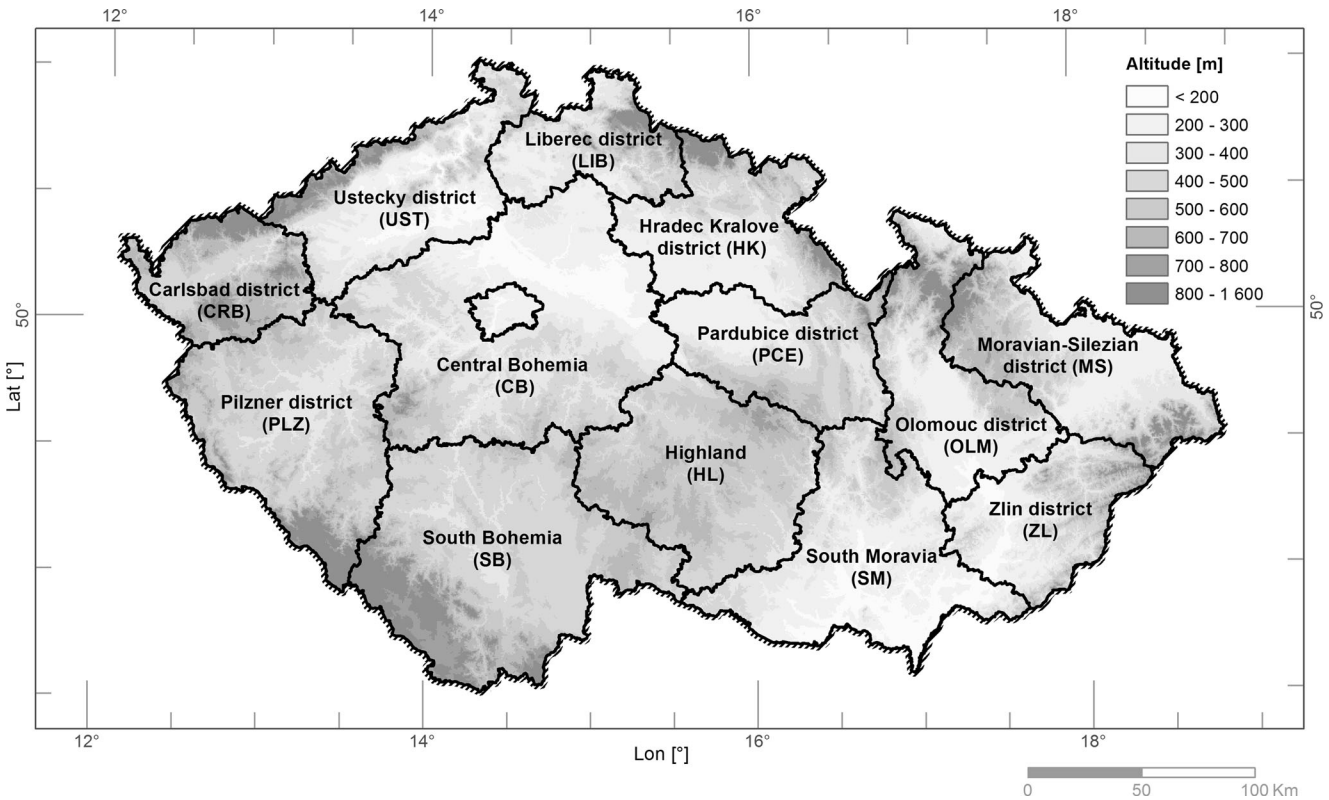

Fig. 1 Map of the Czech Republic with orography and location of districts

points are described, analyzed, and discussed in details in numerous studies (e.g., Barriopedro et al. 2011; Bartholy and Pongrácz 2007; Beniston and Stephenson 2004; Coumou and Rahmstorf 2012; Della-Marta et al. 2007; Fischer and Schär 2010; Schär et al. 2004; Stott et al. 2004). Adverse human health effects of extremely high temperature are partly preventable if appropriate adaptation plans are implemented (Kyselý and Plavcová 2012 and references therein). For adaptation planning, it is necessary to estimate the occurrence of extreme events in the future. In order to assess changes in the occurrence of high air temperature under changing climatic conditions, it is necessary to understand the dynamic causes of these events (Beniston and Stephenson 2004).

Considerable attention has recently been paid to identification of large scale atmospheric conditions leading to extremely high air temperatures in Central Europe. Domonkos et al. (2003) studied the connections between the occurrence of an extremely high air temperature in southcentral Europe during the twentieth century and circulation types (CTs) classified according to Hess and Brezowsky (1977). They found that southerly flow and persistent anticyclonic situations are favorable for high air temperature events. Similarly, according to Porebska and Zdunek (2013), high air temperature events are especially influenced by high pressure blocking situations over western Russia or the Baltic region. Tomczyk and Bednorz (2015) found that occurrence of heat waves over Central Europe is connected to presence of high pressure systems together with positive anomalies of air temperature at 850 hPa level, precipitable water content, and 500 hPa geopotential heights. Della-Marta et al. (2007) confirmed that atmospheric circulation is one of the main factors influencing the occurrence of heat waves over Western Europe. Furthermore, according to Domonkos et al. (2003), the mean residence time of anticyclonic situations is positively correlated with the frequency of an extremely high air temperature. Kyselý (2008) analyzed the relationship between extremely high air temperature events in Central Europe and the persistence of Hess-Brezovsky CTs in more detail. He found that during the twentieth century a longer persistence of CTs was favorable for longer and more severe heat waves.

The focus of the present study is the detection and description of extreme high maximum air temperature events (EXHTEs) over the CZ and the atmospheric circulation leading to their occurrence. There is no unambiguous definition of the extreme temperature event. Many authors, e.g., (Beniston et al. 2007), distinguish three aspects of weather extremity: intensity, rarity, and severity. Intensity and rarity define extremity from a climatic point of view, while severity defines it from an impact point of view (e.g., amount of material losses or number of casualties). Although a single heat wave can kill an incredibly high number of people as in 2003 in France (Cohen et al. 2005), severity is difficult to use in the climatological evaluation of high temperature extremes. The rarity of

a high air temperature value corresponds to its intensity (magnitude) at a given station but it can differ substantially at another station with different climatology (Fig. 2). The geographical region of interest is orographically very complex, and altitude is the main factor influencing air temperature in the CZ (Tolasz et al. 2007), therefore we emphasize the rarity of air temperature values. Moreover, we also consider the spatial extent of the area affected by individual extreme events as well as their duration. To select high air temperature extremes and evaluate their extremity quantitatively, we applied the Weather Extremity Index (WEI). The WEI uses interpolated return periods of station data and optimizes both the considered area and the duration with respect to individual events (Müller and Kašpar 2014). Holtanová et al. (2014) showed that the WEI can be used for identification of extreme high air temperature events and enables their inter-comparison in terms of extremity and spatial extent. Regarding the analysis of large-scale circulation conditions leading to the selected extreme events, we attempted to compile a methodology to describe causal circulation conditions quantitatively and complexly in space. In this respect, the method of anomalies in fields of meteorological variables seems to be an appropriate approach (Cavazos 1999). We assumed, and our previous studies of other weather extremes support the appropriateness of this assumption (e.g., Řezáčová et al. 2005), that there is a close relationship between surface high temperature extremes and the appearance of climatologically high or low values of certain thermo-dynamic variables in specific locations in the free atmosphere. These thermo-dynamic anomalies usually have the extent corresponding to the meso-alpha spatial scale according to Orlanski (1975), i.e., 200–2000 km. They can be described quantitatively in terms of their intensity, extent, and duration (Müller et al. 2009). Such quantitative description enables evaluation of the link between their spatial and temporal distribution and the distribution of extreme events.

The paper is structured as follows: Section 2 comprises a description of the data and methods adopted in our study. The results of the analysis are described and discussed in Section 3. Concluding remarks are presented in Section 4.

2 Data and methods

2.1 Evaluation of high temperature extremes and the weather extremity index

Daily maximum air temperature (TMAX) data from the climatological database of the Czech Hydrometeorological Institute were used for evaluation of temperature extremity and selection of the set of high temperature extremes. Only data from stations with data available for at least 20 years during the period 1961–2010 were employed. The number of stations that met the criteria varied between 134 and 197 during the studied period. First, a regular quality check of the data was carried out. Then, potentially erroneous values were detected using a combination of the following methods: analysis of series of differences between candidate and neighboring stations, i.e., pairwise comparisons, application of limits derived from interquartile ranges, and comparison of the tested series with expected (theoretical) values based on technical series created by means of statistical methods for spatial data (for more details see Štěpánek et al. 2009). On the basis of these methods, erroneous TMAX values were corrected. The data series have not been homogenized.

The rarity of TMAX was evaluated by return periods. The Generalized Extreme Value (GEV) distribution was used as the theoretical distribution of annual maxima of TMAX (Coles 2001) to calculate the return periods. The GEV parameters were estimated using the method of maximum likelihood.

In the next step, the common logarithm of return periods was interpolated into a regular grid with a horizontal resolution of 1 km using local linear regression between the interpolated value and the orography. The common logarithm was used in order to eliminate the exponential nature of the GEV distribution.

Although the area of the CZ is not large, it can happen that an especially high air temperature does not occur over the whole territory during an event. Optimization of the considered area is achieved here by maximizing the variable E_{ta}. First, individual pixels are sorted in decreasing order with respect to the return periods. The pixels are then accumulated into a stepwise increasing area. The variable E_{ta} is defined as a product of the common logarithm of the geometric mean of return periods in the considered area $\log(G_{ta})$ and of the radius of a circle area equivalent to the considered area (R). This relation can be further transformed as

$$E_{ta} = \log(G_{ta})R = \frac{\sum_{i=1}^{n} \log(N_{ti})\sqrt{a}}{n\sqrt{\pi}} \quad (1)$$

where N_{ti} is the return period of the daily temperature maximum (if t=1 day) in a grid point i and a is the area consisting of n grid points. The variable E_{ta} increases initially as we accumulate the pixels with high return periods. The increase decelerates gradually; finally, if there are pixels with significantly lower return periods, the value of E_{ta} starts to decrease. The maximum of E_{ta} represents the extremity of temperature maxima on the given day.

High temperature extremes often last for several days so we also optimized the number of days (t) by searching the time period when E_{ta} reached its maximum in Eq. (1) for t between 1 and 7 days. The maximum of E_{ta} is the WEI value, which represents the extremity of the event. We can now also define the affected area a, the duration t, and the respective geometric mean of return periods G_{ta} in accordance with the relation

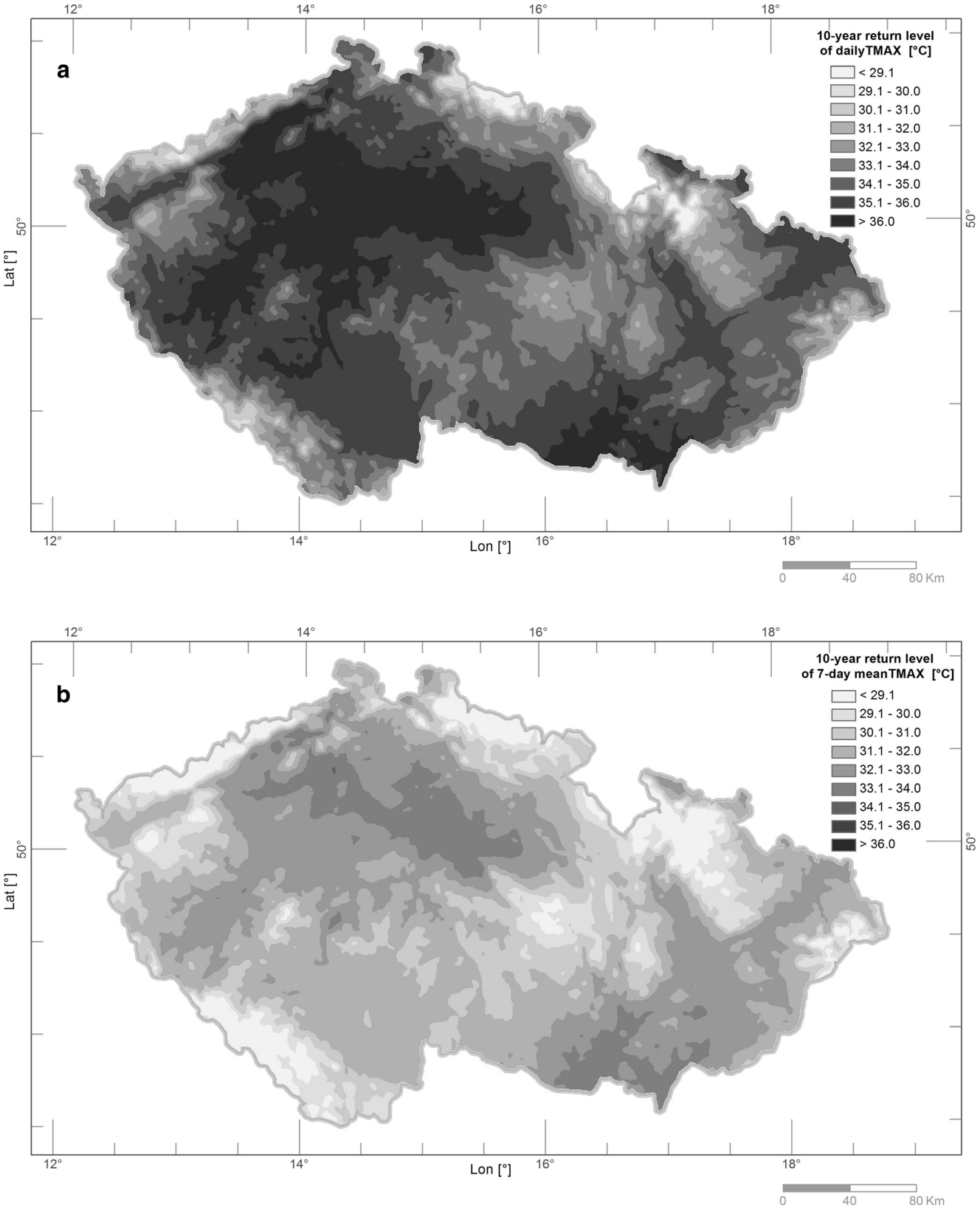

Fig. 2 Ten-year return level of **a** daily TMAX, and **b** 7-day mean TMAX

max(E_{ta})=WEI. For a more detailed description and discussion of the index, see Müller and Kašpar (2014). In the present study, the WEI was calculated for all instances when the return period of daily or 2- to 7-day mean TMAX was higher than

10 years at a minimum of one station. Then, the events with a WEI value of over 50 were chosen as EXHTEs.

The temporal changes in the occurrence of EXHTEs were investigated by the nonparametric Mann-Kendall trend test. The null hypothesis that there is no trend in the time series was tested at the 0.05 significance level. The analyzed time series consisted of annual numbers of EXHTEs in the period 1961–2010.

The central area of an EXHTE was determined as an area with the highest return periods of TMAX exceeding the 90th percentile of the return period over the CZ for the particular event. Thus, the central area of an event can be fragmented into several separate areas. The occurrence of a central area was assigned to all districts (the 14 districts of the territorial division of the CZ were used, see Fig. 1), which were at least partly covered by this area of the highest return periods. Thus, more than one district can be regarded as the central area of a particular EXHTE.

2.2 Synoptic analysis

In order to distinguish synoptic-scale circulation conditions conducive to the reference extreme events, we used 1- to 7-day means of the gridded NCEP/NCAR reanalysis data set with a horizontal resolution of 2.5° (Kalnay et al. 1996).

The technique of detecting a thermo-dynamic anomaly during a reference event is based on assessment of the probability of not exceeding values of the given variable at each grid point. Regarding high values, we applied the GEV distribution using a block maxima approach (for details see Kašpar et al. 2013). The method of maximum likelihood was used for estimating GEV parameters. The probability of not exceeding p of a value $\hat{x}$ is calculated by

$$p\left(\hat{x}\right) = \left[F\left(\hat{x}\right)\right]^{1/(365.2425)} \tag{2}$$

where F denotes the cumulative distribution function of the GEV estimated from annual maxima of daily means in the studied period 1961–2010. Equation (2) assumes the independence of the dataset, which does not have to be fulfilled each time. Nevertheless, this can be neglected because our main purpose was to compare individual events with each other. Regarding low values, we employed the same procedure, but used the reanalysis dataset multiplied by −1 as input. The actual probability of not exceeding these values is equal to $1-p$. The positive and negative anomalies are then a contiguous space characterized by $p \to 1$ and $p \to 0$, respectively.

Causal circulation conditions are naturally rather inhomogeneous, particularly due to the various configurations of the wind field. At first, we therefore classified the reference events into several more homogenous circulation variants. We applied a hierarchical clustering algorithm (e.g., Ward 1963) to the events using the similarity criterion that in addition to air temperature extremity also takes the configuration of the wind field into account. We introduced a vector variable $\mathbf{T}_W$ with the direction parallel to direction of the wind vector $\mathbf{v}$ and with the magnitude equal to air temperature T:

$$\mathbf{T}_W = \frac{\mathbf{v}}{|\mathbf{v}|} \cdot T \tag{3}$$

Westerly and southerly components of $\mathbf{T}_W$ are considered positive while easterly and northerly components of $\mathbf{T}_W$ are deemed negative. The events were then clustered according to the proximity of p of mean values of zonal and meridional components of $\mathbf{T}_W$ in a given period. For the sake of simplicity, we only considered the values of p at a single selected grid point and therefore the spatial dependence of both components did not have to be taken into account. We tested the performance of several clustering algorithms for a number of horizontal as well as vertical locations of the grid point and for various metrics of the proximity using the cophenetic correlation coefficient (Sokal and Rohlf 1962). This verification approach is based on the comparison of the distance of two objects and the distance between the two clusters that contain those two objects. The coefficient equals the correlation of these two sets of values. The closer the value of the coefficient is to 1, the more accurately the clustering reflects original data. On the basis of the results obtained, we opted for the grid point 15° E and 50° N at 700 hPa level, which corresponds well with the territory of the CZ and the Minkowski distance method (Naber 1992). We also preferred the divisive direction of clustering that first identifies the two most distant events (hereinafter node events) and then assigns each of the remaining events to the nearest one. The common agglomerative clustering was found to be inconvenient because the distance of an event to an existing cluster is generally less than the distance to another event, which impedes the formation of new clusters.

We are aware that the continuous variability of circulation conditions partly hinders any crisp clustering method. Primarily, if the distance of an event to the two most distant events is similar, divisive clustering is generally prone to higher uncertainty. Therefore, in the final step, we applied a simple fuzzy approach and assessed the degree of membership of each event to individual variants. The degree of membership $M_{ij} \in <0; 1>$ of the ith event to the jth variant (cluster B_j) is calculated as

$$M_{ij} = \frac{D_{ij} - D_i}{\sum_{k=1}^{m} (D_{ik} - D_i)} \tag{4}$$

where all differences in either the numerator or the denominator that result in a negative value are set to zero. In Eq. (4), D_{ij}

is the inverse value of the normalized total distance of the rth event to all the events in cluster B_j and D_i is the inverse value of the normalized total distance of the ith event to all the reference events divided into m clusters (for details see Kašpar and Müller 2010). It is evident that the less the total distance of an event to those from a particular cluster in comparison with the total distance to all events, the higher the membership degree of the event to the cluster. The main circulation variants and their typical anomalies are discussed in Section 3.2. The climatology of causal circulation conditions in Section 3.3. was evaluated at the grid point 15° E and 50° N and at the 700 hPa level using air temperature (T700) and wind direction as its attributes instead of individual $\mathbf{T}_W$ components.

3 Results and discussion

3.1 High temperature extremes

The occurrence of high air temperature extremes in the CZ is usually connected with a flow of tropical air to Central Europe. A long period with air temperature higher than normal often precedes the occurrence of EXHTE (Krška and Munzar 1984). As the duration of EXHTE varies, we focused on events with a length of 1 to 7 days. As described in Section 2, the WEI calculation threshold is the return period equal to or higher than 10 years. Figure 2 illustrates the 10-year values of daily and 7-day mean TMAX. Naturally, the geographical distribution of the 10-year value is analogous to the distribution of observed TMAX. The highest 10-year TMAX is found in lowland areas of central Bohemia and southern Moravia, with daily (7-day mean) values reaching 38 °C (35 °C). In contrast, the lowest values, 26 °C (21 °C) for daily (7-day mean) TMAX, occur in mountains near the borders of the CZ. The lapse rate of 10-year values of 1- to 7-day TMAX is about 0.8 °C per 100 m.

On the basis of the WEI, 37 extreme high maximum air temperature events lasting from 1 to 7 days were chosen. The frequency of the selected EXHTEs in individual decades during the period 1961–2010 is shown in Fig. 3a. Although the number of events in 1991–2000 and 2001–2010 is higher than in previous decades, the Mann-Kendall test does not indicate any significant trend in annual frequency of EXHTEs. Figure 3b reveals that in the 1960s events of low extremity but with a varying areal extent were recorded. In the 1970s, the EXHTEs had a large areal extent but the extremity was not high. After the year 2000, spatially extensive events were observed in most cases.

As is apparent from Fig. 3c, the EXHTEs in the CZ are most frequent in the second half of July and at the beginning of August. Although less frequent, they were also recorded in June and the second half of August (Holtanová et al. 2014). The value of the highest TMAX for individual events is in the range of 35 to 40 °C, and the daily mean air temperature in locations with the highest TMAX is between 22 and 32 °C. The mean deviation from the 1961–1990 daily normal for the day and place with recorded absolute TMAX for individual events is about 13 °C for TMAX and above 8.4 °C for daily mean air temperature. The EXHTEs are usually ended by a cold front with heavy precipitation.

The frequency of EXHTEs' central area occurrence in the CZ is not evenly distributed. It is most frequent in the south and southwest of Bohemia (SB and PLZ districts) as well as in central Bohemia. Central areas are least frequent in the north and northeastern part of Bohemia (LIB and HK districts) (Fig. 4). The differences in individual decades were assessed to evaluate the temporal evolution of spatial distribution of the occurrence frequency of the central area of high temperature events in the period 1961–2010. The frequency distribution of central area occurrence differs between decades in this period (Fig. 4). While in the first three decades (i.e., 1961–1970, 1971–1980, and 1981–1990) the central areas were most frequent in the central and southern parts of Bohemia, in the 1990s apart from two regions in the western part of the CZ (PLZ and SB districts) the region of highest frequency moved to the ZL and SM districts in southeastern Moravia. In the last decade, 2001–2010, the differences in central area occurrence between the western and eastern part of the CZ were less pronounced.

Circulation conditions naturally vary during individual EXHTEs. As our intention is to identify the main variants of synoptic-scale circulation conditions during high temperature extremes, it is necessary to divide some longer events into more synoptically homogenous short-term episodes. For this purpose, we applied the hierarchical fuzzy clustering algorithm described in Section 2.2 to single days and divided the EXHTEs into episodes with homogenous circulation conditions. In this way, we obtained 53 episodes. Because the WEI for some of these episodes was very low, we used only 47 episodes with sufficiently high WEI in further analysis.

3.2 Variants of synoptic conditions producing high temperature extremes

We identified the main variants of synoptic-scale circulation conditions during high temperature extremes by application of the hierarchical fuzzy clustering algorithm described in Section 2.2 to the 47 episodes presented in Section 3.1. We decided to use two-level divisive clustering, leading to four consistent clusters of single days or episodes. Higher level clusters proved unsuitable for our purposes because of their relatively small number of members. In addition, most of them could not be unambiguously interpreted in terms of synoptic–dynamic meteorology. The final dendrogram tree of 47 episodes is depicted in Fig. 5.

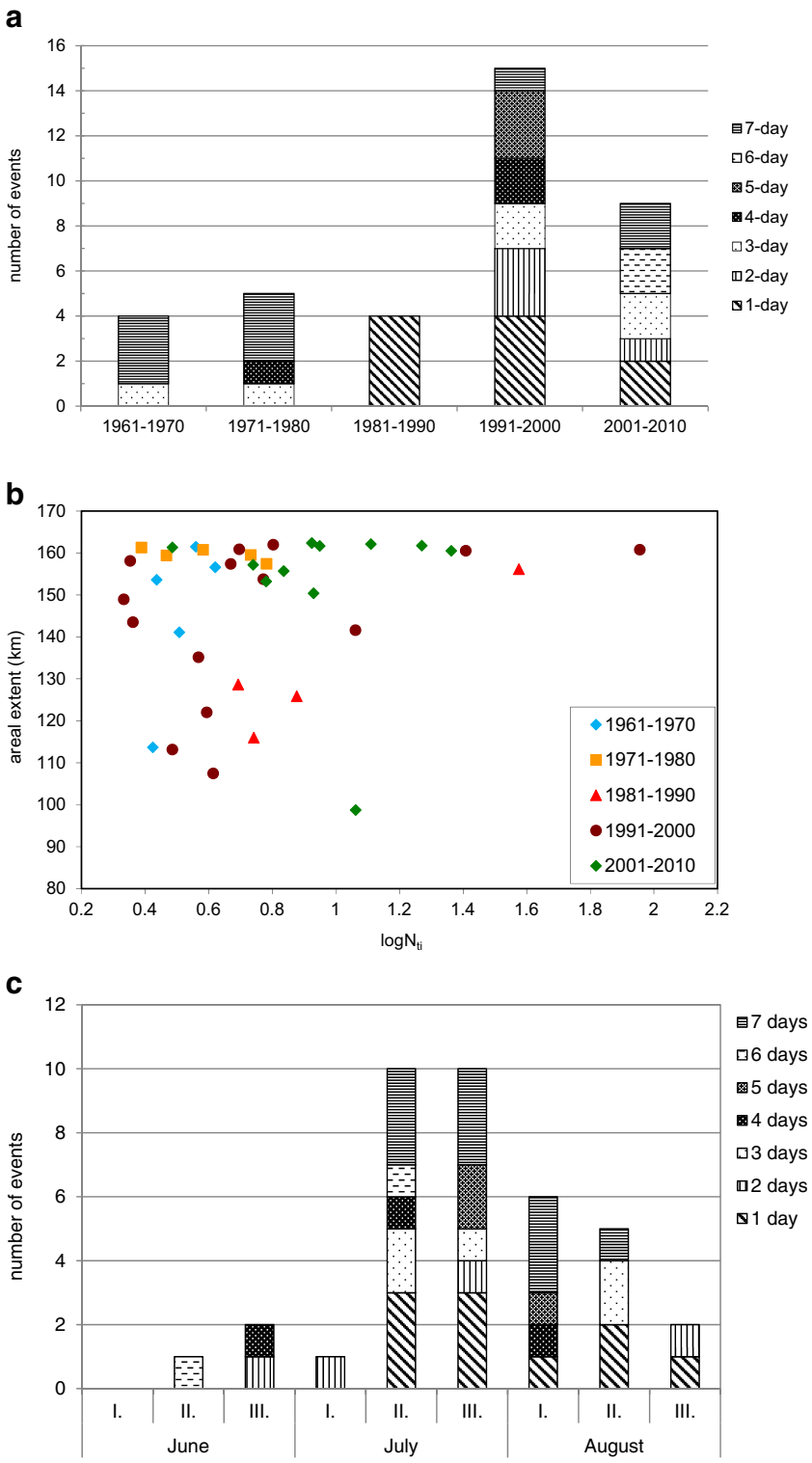

Fig. 3 **a** Frequency of 1- to 7-day events in the period 1961–2010. **b** Distribution of WEI components of all selected extreme events in the period 1961–2010. **c** Frequency of 1- to 7-day events in individual 10-day sections in the summer season

As mentioned above, we further focused on four clusters of episodes, B_1 to B_4, identified in the second level of divisive clustering. These clusters determine four variants of causal circulation patterns. Typical synoptic–dynamic attributes of each variant can be described using the mean thermobaric field and the mean anomalies of the vector variable $\mathbf{T}_w$ defined by Eq. (3) for episodes with a non-zero membership degree to the corresponding cluster. Figure 6 indicates that all variants are related to the middle-troposphere advection of very warm air originating from the Mediterranean, northern Africa, and

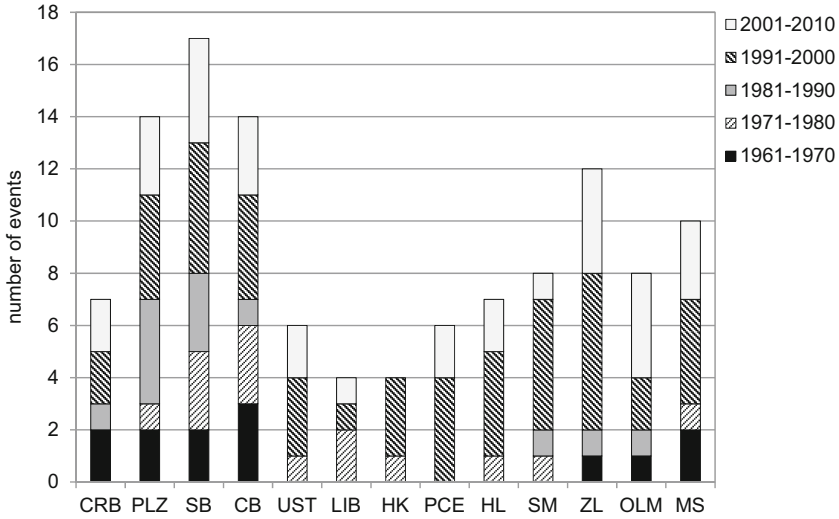

Fig. 4 Spatial distribution of occurrence frequency of the central area of high temperature events in the CZ in the period 1961–2010 with indication of decades. See Fig. 1 for explanation of the abbreviations of individual districts

southeastern Europe. On the other hand, individual variants differ from each other, particularly in the direction of the advection. The most frequent variant B_1 (Fig. 6) is characterized by the westerly flow associated with a high pressure ridge extending from the southwest over Central Europe or with an anticyclone centered to the south. The variant B_2 is characterized by a southwesterly flow between a trough over Western Europe and a ridge of high pressure or an anticyclone to the east. Anomalies in the variable $\mathbf{T}_w$ are the strongest on average because causal circulation conditions are often associated with an approaching cold front and the maximum warm advection ahead of it. The indirect flow of warm air from the north is typical of the variant B_3. Warm air flows around the ridge or an anticyclone to the west and reaches Central Europe along their front side. Finally, the least frequent variant B_4 (Fig. 6) is characterized by an easterly flow between a high pressure area to the northeast and a low pressure area to the southeast. This variant is often associated with the inflow of unstable air masses and the diurnal maximum of convection. It is clear that the presented variants are not always accompanied by high temperature extremes, although it can be expected that the probability of their occurrence increases with the strength of the anomalies in $\mathbf{T}_w$.

The advantage of the applied fuzzy approach over the non-fuzzy approach is well evident for some of the node episodes indicated in Fig. 5. The node episodes EB_1 to EB_4 delimit the clusters B_1 to B_4, respectively. However, their membership degree to these clusters is not always 100 %. The membership degree of the node episode EB_2 to the cluster B_2 is 61 %, while that of the node episode EB_4 to the cluster B_4 is only 56 %. This is due to the fact that in general, node episodes are not necessarily representative of episodes in corresponding

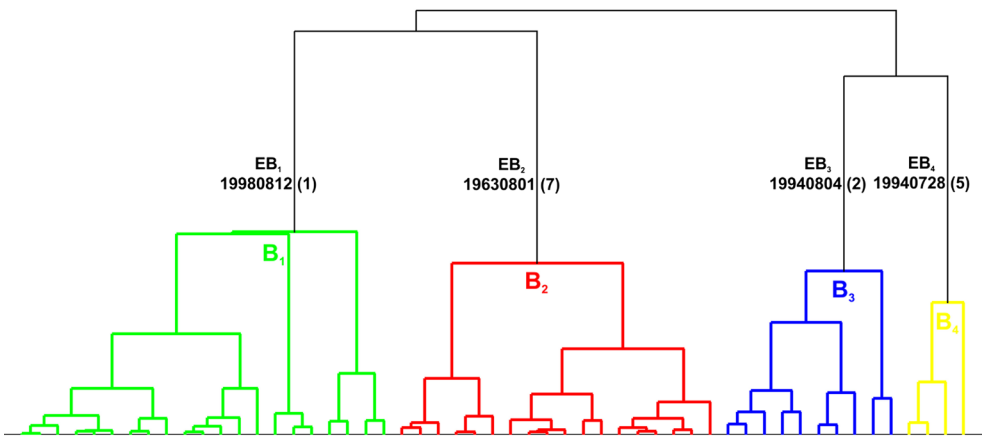

Fig. 5 Dendrogram plot resulting from divisive clustering of 53 reference episodes of high temperature extremes. The length of vertical segments is proportional to the Minkowski distance between the clusters and/or individual episodes. Four clusters identified in the second level of divisive clustering define synoptic-scale circulation variants and are marked B_1 to B_4. The most distant (node) episodes in each of the two clusters identified in the first level of divisive clustering are indicated by their *abbreviation*, their onset (in the format yyyymmdd) and duration in days (in *brackets*)

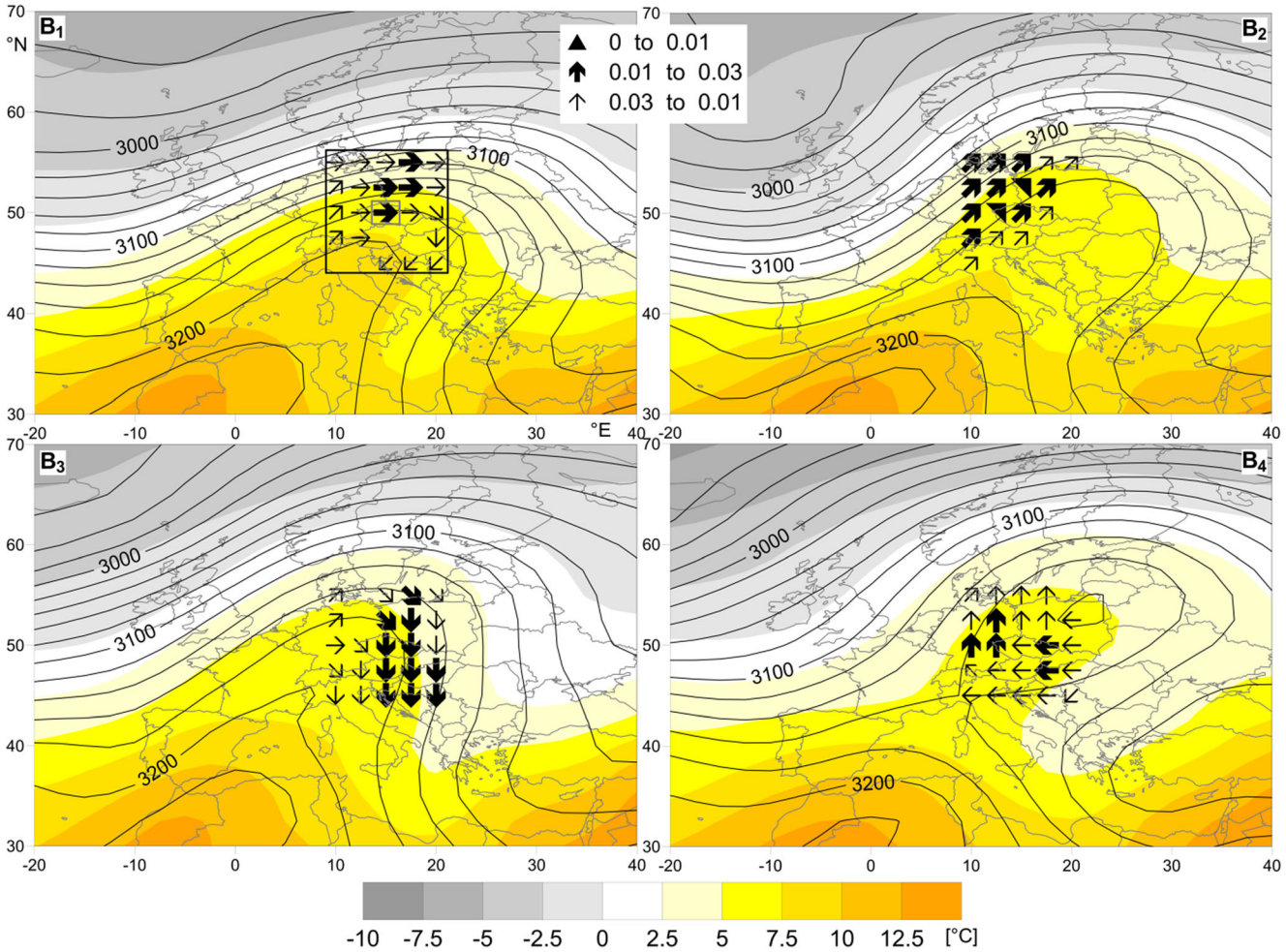

Fig. 6 Mean geopotential height, air temperature, and extremity of $\mathbf{T}_w$ components (see Eq. (3)) at the 700 hPa level during episodes representing individual clusters B_1 to B_4 (see Fig. 5). *Black contours and colors* correspond to the weighted arithmetic mean of geopotential height (m) and temperature (°C) fields, respectively. *Black arrows* correspond to the minimum weighted geometric mean of probabilities of exceeding the magnitude of $\mathbf{T}_w$ components in cardinal and intercardinal directions according to the legend. Applied weights equal membership degrees of individual episodes to the cluster. In the top left figure, the *black square* shows the domain where the mean probability is computed. The *gray square* shows the grid point used in clustering

clusters resulting from the divisive direction of the clustering. Similar membership degrees of episodes EB_2 as well as EB_4 to the clusters B_2 and B_4 can be explained by their similar distance to the node episodes that delimit the initial two clusters identified in the first level of divisive clustering. Inspection of Fig. 7 confirms that the episodes EB_2 and EB_4 have features of both circulation variants B_2 and B_4 with prevailing south to southeast causal warm advection.

3.3 Climatology of extreme episodes and their synoptic variants

The frequency of extreme episodes distinguished by synoptic variants in individual decades in the period 1961–2010 is shown in Fig. 8a. While the episodes associated with synoptic variants B3 and B4 are quite evenly distributed, a considerable increase of episodes connected with B1 and B2 variants was recorded in the last two decades. Concerning seasonality, the B3 and B4 episodes only occur from the second 10-day period of July to the first 10-day period of August, whereas the B1 and B2 episodes can sometimes, albeit rarely, be recorded at the beginning and end of summer (Fig. 8b).

When we compare the synoptic variants based on the WEI of detected EXHTEs, the highest WEI value was recorded for the B4 episode, which lasted for 5 days from 28 July to 1 August 1994 and affected nearly all the territory of the CZ. The TMAX value was between 34 and 39 °C in lowlands and between 24 and 30 °C in the mountains. The highest TMAX reached the value 39.2 °C with a return period of 50 years. The absolute maximum of TMAX for the period 1961–2010, 40.2 °C with a return period of about 100 years, was recorded on 27 July 1983 at the Prague-Uhříněves station during the B1

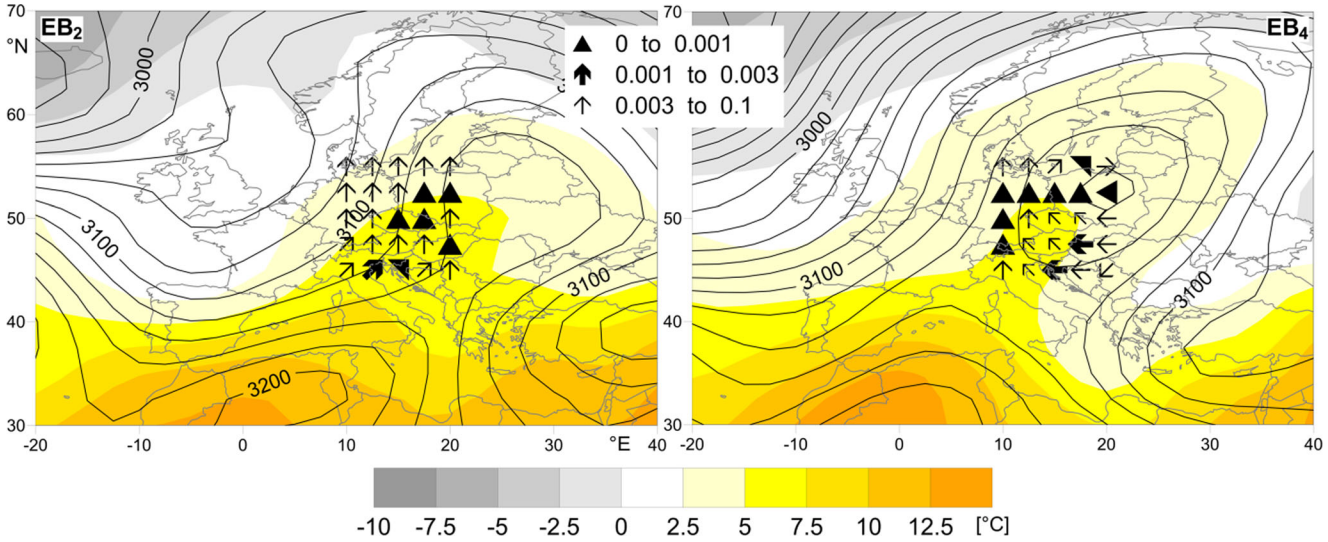

Fig. 7 Same as Fig. 6, but for the node episodes EB_2 and EB_4

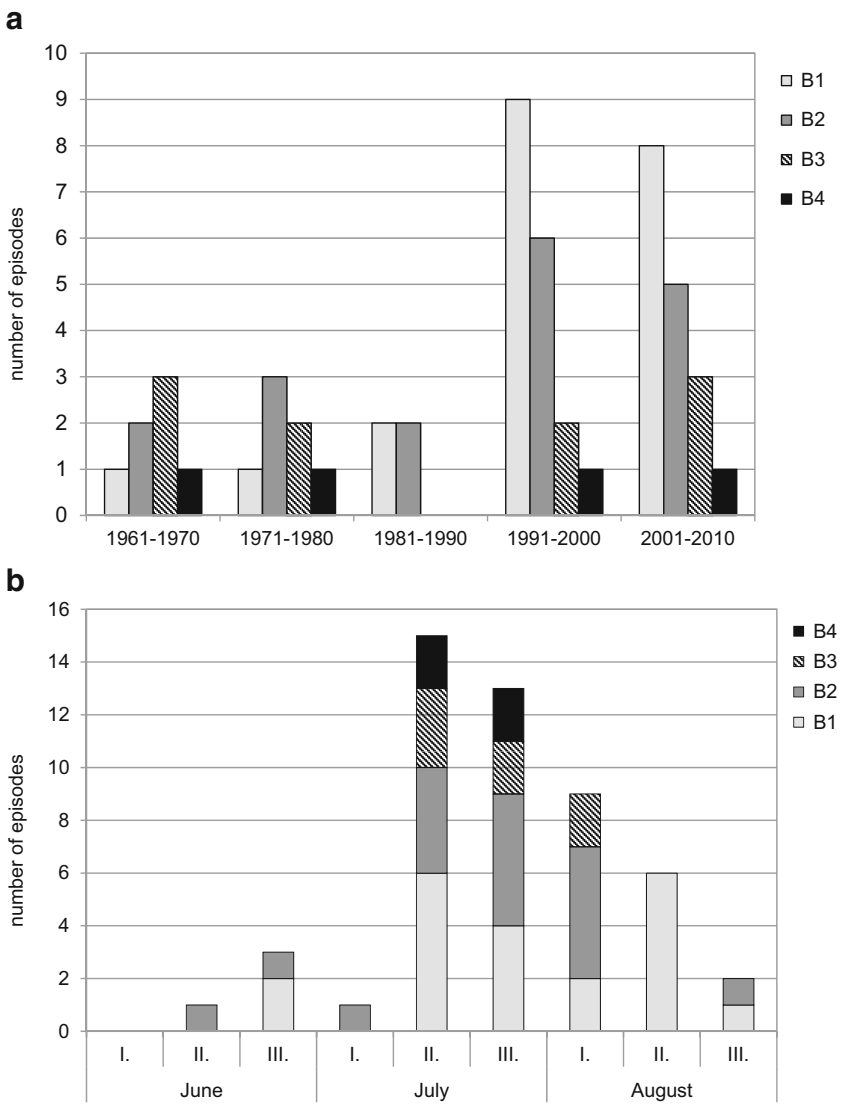

Fig. 8 **a** Frequency of extreme episodes distinguished by synoptic variants (B1 to B4) in individual decades in the period 1961–2010. **b** The frequency of extreme episodes distinguished by synoptic variants (B1 to B4) in individual 10-day sections in the summer season

episode with the second highest WEI. The most extreme episodes connected with B2 and B3 variants were less strong in terms of the WEI.

The extreme episodes usually affect a large part of the CZ and in fact often exceed the studied region but there are regional differences in their extremity depending on causal synoptic-scale circulation conditions. Figure 9 shows how the characteristic spatial distribution of episode centers varies among individual circulation variants. First, the southeastern part of the CZ is almost always affected when the B1 and B2 variants occur. For instance, all events centered in the SM district were connected with either B1 or B2 episodes. In contrast, episodes connected with the B3 and B4 variants usually affect the northwestern part of the CZ. For instance, 80 % of the centers of B3 episodes were recorded in the KV and PLZ districts. The results are in accordance with the position of the warm air ridge, which shifts more to the west and north for the variants B3 and B4 in comparison with the variants B2 and B1, respectively.

The climatology of casual circulation conditions was studied by the evaluation of high quantiles of T700 because near surface air temperature maxima are correlated with T700 maxima. The 1-day average of T700 was higher than the 95th percentile (4 °C) on all but two days with $WEI > 50$. Moreover, when considering several day events as a whole, 1-day T700 was almost always higher than the 99th percentile (6.3 °C) for at least one day. Therefore, we studied sets of T700 values above the 95th percentile (913 values), 99th percentile (183 values), and 99.9th percentile (18 values) for each of the 1- to 7-day periods between 1961 and 2010. Only independent, i.e., not overlapping or adjacent, periods were considered. In addition, we selected the maximum of T700 from overlapping and adjacent periods. We particularly studied the seasonal distribution and changes in the frequency of high T700 values between 1961 and 2010. From the point of view of temporal development, the twofold increase in the number of cases with T700 above the 95th and 99th percentiles was observed during the second half of the monitored period. This is in accordance with the increase in the mean temperature and its variability in Central Europe (Schär et al. 2004). In contrast, the sets of T700 above the 99.9th percentile show no or even the opposite trend. For example, from 13 independent maxima of 1-day T700, only 3 occurred after the year 1985. It seems that the temporal distribution of T700 values with high return periods is mainly affected by coincidental circulation anomalies that cause these extremes.

Regarding seasonality, T700 values above the 95th and 99th percentile were recorded from the beginning of May to the beginning of November and from the end of May to the middle of October, respectively. With regard to values above the 99.9th percentile, the period of occurrence decreased, lasting from the middle of June to the middle of September. This more or less corresponds to the period of the EXHTEs occurrence; however, the presence of T700 extremes in September is surprising in this respect. While relatively less frequent in the set, they can reach very high values (e.g., the absolute maximum of 5-day T700 on 16–20 September 1961). In such cases, the near surface TMAX values are also quite high in respect of the annual course, but not in comparison with annual maxima and therefore are not identified as EXHTEs according to our criteria. A possible explanation is the decrease in radiative surface warming at the turn of summer and autumn, while higher air layers can still be affected by the advection of very warm air from south and west sectors. No EXHTE was found in September during the investigated period 1961–2010 in our study. However, it is worth mentioning that an event with very high maxima in a large part of Central Europe was recorded in the second 10-day period of September 1947.

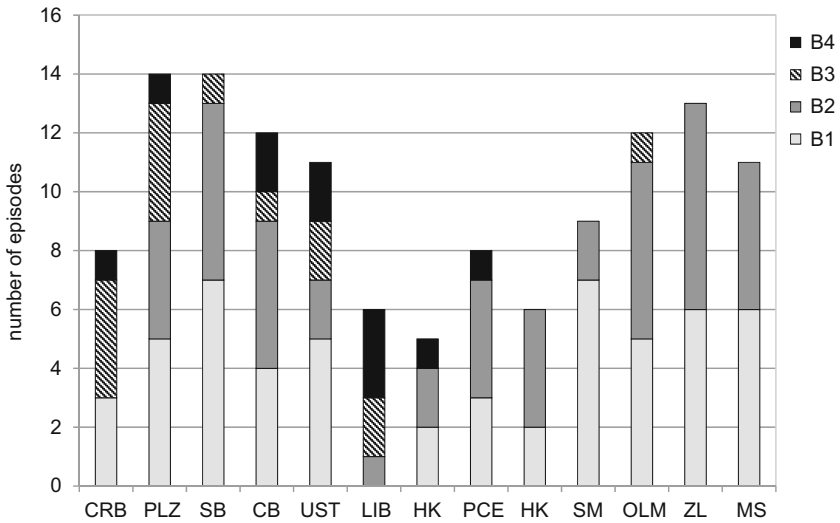

Fig. 9 Occurrence frequency of episode centers distinguished by synoptic variants (B1 to B4) in individual districts of the CZ in the period 1961–2010. See Fig. 1 for explanation of the abbreviations of individual districts

4 Concluding remarks

We analyzed the connection between EXHTEs and circulation anomalies based on a sample of EXHTEs selected according to WEI values. The WEI evaluation, which incorporates both the extremity and spatial extent of TMAX, is based on an unprecedented amount of meteorological data. To our knowledge, there has not been any similar study incorporating all station measurements from the area of the CZ available in the Czech Hydrometeorological Institute database. In Holtanová et al. (2014), it was shown that the WEI is useful for identification and inter-comparison of EXHTEs, but may not detect all events with a relatively high TMAX value but low return periods that persist for a longer time. We were concerned with weather extremes rather than climate extremes as distinguished by Diaz and Murnane (2008), thus only studied time periods up to 7 days, which means that we might not have covered all EXHTEs with potentially severe impacts in various sectors.

Four variants of atmospheric circulation connected with episodes of high temperature extremes were identified based on anomalies of 700 hPa air temperature and wind field. The synoptic-scale circulation conditions of individual variants do not differ considerably. All variants are connected with a high pressure ridge extending from the southwest over Central Europe and a low pressure area in the eastern Mediterranean. Individual variants differ from each other particularly in the direction of advection (Fig. 6). The most extreme high air temperature events are connected to variant B4 (the least frequent) characterized by an easterly flow and to variant B1 (the most frequent) characterized by a westerly flow. The variant B4 corresponds to the occurrence of a blocking anticyclone above the Baltic region, which was described by Porebska and Zdunek (2013) as favorable for an extreme high air temperature in Central Europe. The relation between the central area and the synoptic variant of EXHTE was found. The southeastern part of the CZ is affected when the variants B1 and B2 occurred, while the central area of episodes connected with the variants B3 and B4 were usually located in the northern and western parts of the CZ. The results are in accordance with the position of the warm air ridge, which shifts more to the west and north for the variants B3 and B4 in comparison with the variants B2 and B1, respectively.

We selected 37 EXHTEs from the period 1961–2010 with a duration of 1 to 7 days. The most frequent occurrence of EXHTEs was in 1991–2000, and a high number was also recorded in 2001–2010. However, no statistically significant temporal trend in EXHTE occurrence was found. A great increase of episodes of high temperature extremes connected with variants B1 and B2 was recorded in the last two decades. It corresponds with the shift of the central area of EXHTEs to the eastern part of the CZ. It should be kept in mind that EXHTEs usually affect a more extensive area than the CZ, which was considered in this study. However, our results are in accordance with Lhotka and Kyselý (2014), who analyzed extreme temperature events in the whole of Central and Eastern Europe. Even the most extreme event in terms of WEI in July/August 1994 was also identified as the most extreme by Lhotka and Kyselý (2014).

The highest frequency of EXHTEs was observed in July and the first half of August, with a lower frequency in June and the end of August. The occurrence of EXHTEs outside the main season has been observed only since 1992 but not before. The extremity of these events is comparable with the extremity of EXHTEs during the main season. An example is the EXHTE in the second half of August 2012, where the highest TMAX on record in the CZ (40.4 °C) occurred (Holtanová et al. 2014). Between 1961 and 2010, practically no EXHTEs occurred in September. This more or less corresponds to the period when extremes in the 700 hPa air temperature occur. However, extremes in the 700 hPa air temperature were also recorded in September. A possible explanation is the decrease in radiative surface warming at the turn of summer and autumn, while higher air layers can still be affected by advection of very warm air from the south and west sectors. For detection of anomalies in near surface air temperature corresponding to autumn extremes at the 700 hPa level, it would be necessary to remove the annual air temperature cycle. However, this is beyond the scope of the present paper.

Acknowledgments The observed data of daily maximum air temperature were provided by the Czech Hydrometeorological Institute. The work has been supported by grant P209/11/1990 funded by the Czech Science Foundation.

References

Bartholy J, Pongrácz R (2007) Regional analysis of extreme temperature and precipitation indices for the Carpathian Basin from 1946 to 2001. Glob Planet Chang 57(1–2):83–95

Barriopedro D, Fischer EM, Luterbacher J, Trigo RM, Garcia-Herrera R (2011) The hot summer of 2010: redrawing the temperature record map of Europe. Science 332:220–224

Belda M, Holtanová E, Halenka T, Kalvová J (2014) Climate classification revisited: from Köppen to Trewartha. Clim Res 59:1–13. doi:10.3354/cr01204

Beniston M, Stephenson DB (2004) Extreme climatic events and their evolution under changing climatic conditions. Glob Planet Chang 44:1–9. doi:10.1016/j.gloplacha.2004.06.001

Beniston M, Stephenson DB, Christensen OB, Ferro CAT, Frei C, Goyette S, Halsnaes K, Holt T, Jylha K, Koffi B, Palutikof J, Scholl R, Semmler T, Woth K (2007) Future extreme events in European climate: an exploration of regional climate model projections. Clim Chang 81:71–95. doi:10.1007/s10584-006-9226-z

Brázdil R, Chromá K, Dobrovlný P, Tolasz R (2009) Climate fluctuations in the Czech Republic during the period 1961–2005. Int J Climatol 29:223–242. doi:10.1002/joc.1718

Cavazos T (1999) Large-scale circulation anomalies conducive to extreme precipitation events and derivation of daily rainfall in Northeastern Mexico and Southeastern Texas. J Clim 12:1506–1523

Cohen JC, Veysseire JM, Bessemoulin P (2005) Bio-climatological aspects of summer 2003 over France. In: Extreme weather events and public health responses. Springer, pp. 33–45. DOI: 10.1007/3-540-28862-7_4

Coles S (2001) An introduction to statistical modeling of extreme values. Springer Verlag, London. ISBN 1-85233-459-2

Coumou D, Rahmstorf S (2012) A decade of weather extremes. Nat Clim Chang 2:491–496

Della-Marta PM, Luterbacher J, von Weissenfluh H, Xoplaky E, Brunet M, Wanner H (2007) Summer heat waves over Western Europe 1880–2003, their relationship to large scale forcing and predictability. Clim Dyn 29:251–275

Diaz HF, Murnane RJ (2008) The significance of weather and climate extremes to society: an introduction. In: Climate extremes and society. Cambridge University Press, Cambridge, UK, pp 1–7. doi:10.1017/CBO9780511535840.003

Domonkos P, Kyselý J, Piotrowicz K, Petrovic P, Likso T (2003) Variability of extreme temperature events in south-central Europe during the 20th century and its relationship with large-scale circulation. Int J Climatol 23:987–1010

Fischer EM, Schär C (2010) Consistent geographical patterns of changes in high-impact European heatwaves. Nat Geosci. doi:10.1038/NGEO866

Hess P, Brezowsky H (1977) Katalog der Grosswetterlagen Europas 1881–1976. Berichte des Deutschen Wetterdienstes, 113. Deutscher Wetterdienst, Offenbach a. Main

Holtanová E, Valeriánová A, Crhová L, Racko S (2014) Heat wave of August 2012 in the Czech Republic: comparison of two approaches to assessment of high temperature events. Stud Geophys Geod. doi:10.1007/s11200-014-0805-6, **10/2014**

Kalnay E, Kanamitsu M, Kistler R, Collins W, Deaven D, Gandin L, Iredell M, Saha S, White G, Woollen J, Yhu Y, Chelliah M, Ebisuzaki W, Higgins W, Janowiak J, Mo KC, Ropelewski C, Wang J, Leetmaa A, Reynolds R, Jenne R, Joseph D (1996) The NCEP/NCAR 40-year reanalysis project. Bull Am Meteorol Soc 77(3):437–471

Kašpar M, Müller M, Pecho J (2013) Comparison of meteorological conditions during may and august 2010 floods in Central Europe. AUC Geographica 48(2):27–34

Kašpar M, Müller M (2010) Variants of synoptic-scale patterns inducing heavy rains in the Czech Republic. Phys Chem Earth 35:477–483

Krška K, Munzar J (1984) Special temperature conditions of tropic summer in ČSSR and in Europe. In Czech Meteorologické zprávy 37

Kyselý J (2008) Influence of the persistence of circulation patterns on warm and cold temperature anomalies in Europe: analysis over the 20th century. Glob Planet Chang 62:147–163

Kyselý J (2010) Recent severe heat waves in Central Europe: how to view them in a long-term prospect? Int J Climatol 30:89–109

Kyselý J, Plavcová E (2012) Declining impacts of hot spells on mortality in the Czech Republic, 1986–2009: adaptation to climate change? Clim Chang 113:437–453. doi:10.1007/s10584-011-0358-4

Lhotka O, Kyselý J (2014) Characterizing joint effects of spatial extent, temperature magnitude and duration of heat waves and cold spells over Central Europe. Int J Climatol. doi:10.1002/joc.4050

Müller M, Kašpar M (2014) Event-adjusted evaluation of weather and climate extremes. Nat Hazards Earth Syst Sci, in press.

Müller M, Kašpar M, Řezáčová D, Sokol Z (2009) Extremeness of meteorological variables as an indicator of extreme precipitation events. Atmos Res 92(3):308–317

Naber GL (1992) The geometry of Minkowski spacetime. Springer, New York

Orlanski I (1975) A rational subdivision of scales for atmospheric processes. Bull Am Meteorol Soc 56:517–530

Porebska M, Zdunek M (2013) Analysis of extreme temperature events in Central Europe related to high pressure blocking situations in 2001–2011. Meteorol Z 22(5):533–540

Řezáčová D, Kašpar M, Müller M, Sokol Z, Kakos V, Hanslian D, Pešice P (2005) A comparison of flood precipitation episode in August 2002 with historic extreme precipitation events on the Czech territory. Atmos Res 77(1–4):354–366

Schär C, Vidale PL, Lüthi D, Frei C, Häberli C, Liniger MA, Appenzeller C (2004) The role of increasing temperature variability in European summer heatwaves. Nature 427:332–336

Sokal RR, Rohlf FJ (1962) The comparison of dendrograms by objective methods. Taxon 11:33–40

Štěpánek P, Zahradníček P, Skalák P (2009) Data quality control and homogenization of air temperature and precipitation series in the area of the Czech Republic in the period 1961–2007. Adv Sci Res 3:23–26

Stott PA, Stone DA, Allen MR (2004) Human contribution to the European heatwave of 2003. Nature 432:610–614

Tolasz R, Míková T, Valeriánová A, Voženílek V (eds) (2007) Climate atlas of Czechia. Czech Hydrometeorological Institute, Prague &Univerzita Palackého, Olomouc

Tomczyk AM, Bednorz E (2015) Heat waves in Central Europe and their circulation conditions. Int J Climatol. doi:10.1002/joc.4381

Trewartha GT, Horn LH (1980) Introduction to climate, 5th edn. McGraw Hill, New York, NY

Ward JH (1963) Hierarchical grouping to optimize an objective function. J Am Stat Assoc 58:236–244